Catalysis Science & Technology

Accepted Manuscript

ROYAL SOCIETY OF CHEMISTRY

www.rsc.org/catalysis

Journal Name

ARTICLE

Highly active and durable Pd/Fe_2O_3 catalysts for wet CO-oxidation under ambient conditions.

Received 00th January 20xx,
Accepted 00th January 20xx

DOI: 10.1039/x0xx00000x

www.rsc.org/

A.S. Ivanova,[a,b*] E.M. Slavinskaya,[a,b] O. A. Stonkus,[a,b,c] R. V. Gulyaev,[a,b] T.S. Glazneva,[a,b] A.S. Noskov,[a] and A. I. Boronin[a,b**]

Pd/Fe_2O_3(FeOOH), catalysts were prepared indifferent ways : *T* – traditional incipient wetness impregnation (IWI) from a solution of palladium nitrate, *D* – modification of the support surface by dimethylformamide (DMF) prior to IWI, and *DF* – variant *D* followed by treatment with a sodium formate solution were examined. These catalysts have been tested for CO oxidation under isothermal conditions at 20°C in the presence ad absence of water vapor and characterized by XRD, TEM, XPS, H_2-reduction and adsorption methods. The Pd(*T*)/Fe_2O_3 catalyst is highly active in CO oxidation at room temperature under "dry" conditions but is deactivated in the presence of water vapor. The Pd(*D*)/Fe_2O_3 catalyst is inactive in low-temperature CO oxidation, whereas Pd(*DF*)/Fe_2O_3(*FeOOH*) catalysts are characterized by high activity at room temperature and ambient humidity. The main state of palladium in the Pd(*T*)/Fe_2O_3 catalyst without pretreatment with DMF is in nitrate complexes, where it can readily be reduced to form clusters ~ 1.5 nm in size. In the case of Pd(*D*)/Fe_2O_3, palladium interacts with dimethylformamide forming complexes, which cannot be reduced by hydrogen at room temperature. It is proposed that palladium clusters are located within the interdomain boundaries of the hydrophobic support in (0.5–1.0)%Pd(*DF*)/Fe_2O_3active catalysts. These (0.5–1.0)%Pd(*DF*)/Fe_2O_3 catalysis were active towards CO oxidation at ambient temperature and humidity during several hours.

Introduction

Carbon monoxide (CO) is a highly toxic gas whose action is based on its ability to bind strongly with blood hemoglobin; this binding proceeds 200–300 times more rapidly compared to oxygen. The resulting carboxyhemoglobin blocks oxygen transport and cellular respiration. The main sources of CO emission to the atmosphere are motor transport, industry, and thermal power stations. Humans suffer from accumulation of CO in enclosed spaces, such as dwellings, working areas, vegetable storage facilities, submarines, and orbital stations. It is especially important to take into account that the permissible exposure limit for carbon monoxide is 55 mg/m^3 [1] while daily CO emission from the human body is about 95–130 mg/day [2]. Thus, low temperature CO oxidation that is performed at room temperature and under ambient humidity is very necessary in these fields and applies certain requirements to the catalysts used in this process. For instance, oxidation of CO in the presence of water vapor may be accompanied by its condensation in micro/mesopores of a hydrophilic support, so the choice of support and conditions of its synthesis are crucial among the factors determining the low-temperature activity of catalysts in CO oxidation. The catalyst's stability towards water vapor can be improved by employing a hydrophobic support, which is obtained by the formation of a carbon-containing component on its surface.

In recent years particular attention has been paid to Au-containing systems, among which Au/Fe_2O_3, Au/Co_3O_4 and Au/TiO_2 showed high activity in room temperature CO oxidation [3]. As reported in [4], a 2.5 at.% Au/Fe_2O_3catalyst synthesized by coprecipitation was highly active in CO oxidation at ~ 30 C in its initial state. However, a common problem is that most of the supported gold catalysts are unstable under long-term reaction conditions and upon storage, especially at a relatively low temperature in the presence of water vapor [5,6].

In addition to Au catalysts, Pd catalysts are also active in the low-temperature oxidation of CO. Depending on the properties of the support, the temperature corresponding to 50% CO conversion (T_{50}) increases in the following order: CeO_2 (45°C) < ZrO_2 (165°C) < TiO_2 (185°C) < Al_2O_3 (205°C) < SiO_2 (255°C) [7]. The authors of [7] believe that the activity of Pd catalysts in CO oxidation is determined by the presence of metallic palladium, while PdO particles have low activity. They suggest that the deposition of less than 2 wt.% Pd is sufficient to form the active sites of CO oxidation. A further increase in Pd content produced only bulk PdO particles, which contributed insignificantly to the catalytic activity. As shown by analysis of the literature, Pd catalysts are less active compared

[a] Boreskov Institute of Catalysis SB RAS, Novosibirsk 630090, Russia
[b] NovosibirskStateUniversity, Novosibirsk 630090, Russia
[c] Research and Educational Center for Energy Efficient Catalysis, NovosibirskStateUniversity, Novosibirsk 630090, Russia
*E-mail:iva@catalysis.ru; Fax: +7 3833308056; Tel: +7 3833269825
**E-mail:boronin@catalysis.ru; Fax: +7 3833308056; Tel: +7 3833269631

to Au-containing ones. However, it should be noted that Au catalysts are more active unless subjected to thermal treatment or dried at a low temperature. This suggests that OH groups can affect activity in CO oxidation. Indeed, it was demonstrated [8] that the use of $Al(OH)_x$, $Fe(OH)_x$ and $Co(OH)_x$ hydroxides as the supports for Pd catalysts made it possible to increase the catalytic activity in CO oxidation: T_{50} was ca. 140 and 78°C for $Pd/Al(OH)_x$and $Pd/Co(OH)_x$containing4.0 wt% Pd, respectively. In this case, the activity of $Pd/Fe(OH)_x$ was comparable with that of the $Au/Fe(OH)_x$ catalyst with a similar content of a noble metal. Stability tests of 4.1 wt% $Pd/Fe(OH)_x$ showed that the catalyst ensured complete conversion of CO, which was retained for 10 h at 0°C and 210 h at 20°C. However, the palladium content was quite high. In addition, data on the activity were obtained for the oxidation of CO in a "dry" mixture containing no water vapor. At the same time, it is known that the presence of water exerts a detrimental effect on the catalytic activity. Deactivation of the catalyst can be attributed to the transformation of bicarbonate intermediates into inactive carbonates that block the active surface sites [9]. Thus, catalysts that efficiently operate in the oxidation of CO at room temperature under ambient humidity are of great interest.

The present study was carried out with catalysts containing less than 1 wt.% Pd supported on ferric oxide or hydroxide (Fe_2O_3 or FeOOH). Their catalytic activity is known to depend not only on the properties of the noble metal and support, but also on the method of active component deposition. The chosen catalysts are intended for the oxidation of CO not only in the absence but also in the presence of water vapor in the reaction mixture, so the support surface was modified with dimethylformamide (DMF) – $[HCON(CH_3)_2]$ containing two hydrophobic groups.

This work aimed to reveal the effect of the iron-containing support, the content of palladium and the synthesis procedure on the physicochemical and catalytic properties of Pd/Fe_2O_3(FeOOH) catalysts in CO oxidation at the room temperature in the presence and absence of water vapor in the reaction mixture.

Experimental

Preparation of the catalysts

The preparation of a ferric hydroxide support by precipitation of iron nitrate solution with an aqueous solution of ammonia at pH 8.5±0.1 and room temperature for 2 h. The resulting suspension was filtered; the precipitate was washed with distilled water and dried first in air at room temperature and then at 110°C for 12–14 h to obtain ferric hydroxide (FeOOH). Thermal treatment of the FeOOH at 450°C led to the formation of ferric oxide (Fe_2O_3).

The deposition of palladium via:

- the impregnation of ferric oxide, which was pretreated with a solution of dimethylformamide $[HCON(CH_3)_2]$ (D) to introduce the carbon-containing component, with a palladium nitrate solution followed
- either by drying to obtain a catalyst denoted as $Pd(D)/Fe_2O_3$;
- or by treatment with a solution of sodium formate (F) at 80°C, filtering, washing and drying to obtain a catalyst denoted as $Pd(DF)/Fe_2O_3$(FeOOH).
- the impregnation of ferric oxide with a palladium nitrate solution followed by drying to obtain the reference catalyst denoted as $Pd(T)/Fe_2O_3$, T – traditionally.

Palladium loading was 0.1–1 weight %. The specified palladium content in the investigated catalysts is presented in table 1.

Methods of investigation

Atomic absorption spectrometry was used to determine the concentrations of the main components to an accuracy of 0.01 – 0.03% [10].

X-ray diffraction (XRD) studies were carried out using a D-500 (Siemens, Germany) diffractometer with CuK_α (λ = 1.5418 Å) monochromatic radiation. The diffraction profiles were recorded both in a continuous mode and in a step-by-step scanning mode at 0.05–0.1° 2Θ steps with a dwell time of 20–30 s depending on the sample's crystallinity. The phases were identified by comparison of the measured set of interplanar distances di and the corresponding intensities of the diffraction maxima Ii with those found in the JCPDS database (PCPDF Win. Ver. 1.30, JCPDS ICDD, Swarthmore, PA, USA, 1997).

High resolution transmission electron microscopy (HRTEM) images were obtained using a JEM-2010 electron microscope (JEOL Ltd., Japan) with a lattice-fringe resolution of 0.14 nm at an accelerating voltage of 200 kV. The high-resolution images of periodic structures were analyzed by the Fourier method. Local energy-dispersive X-ray analysis (EDXA) was carried out using an EDX spectrometer (EDAX Inc.) equipped with a Si (Li) detector with a resolution of 130 eV. The samples for the HRTEM study were prepared on perforated carbon film mounted on a copper grid.

Fourier transform infrared (FT-IR) spectraof adsorbed CO were registered on a Shimadzu FTIR-8300 spectrometer in the range of 400-6000 cm-1 with a resolution of 4 cm-1 and a number of scans of 100. The sample was pressed into a pellet (1x2 cm2 in size and 40-50 mg in weigh) without a binder, placed in an IR cell, and evacuated for 30 min at room temperature. The adsorption of CO was performed at room temperature and CO pressure of 10 and 20 Torr.

X-ray photoelectron spectroscopy (XPS) studies were carried out using an ES300 electron spectrometer by Kratos Analytical with MgK_α characteristic X-ray radiation (hν = 1253.6 eV). Powdered samples were pressed into pellets and loaded into the spectrometer. The spectra were processed using the special software XPS-Calc, which has been previously used for many other systems [11-13]. The spectra were calibrated against the C1s line of the support, with E_b = 285.0 eV. The chemical composition of the catalysts was calculated using the integral intensities of the lines or their components, subject to the atomic sensitivity factors reported in [14].

Ar adsorption–desorption isotherms were obtained with SORP-4.1 and the SBET method [15] was applied to calculate the total surface area with an accuracy of ± 10%.

Reduction by hydrogen at room temperature (H_2-reduction). Prior to the H_2-reduction study, the initial catalyst was treated in a helium flow to remove water and carbonates from the surface. After that, a mixture containing 0.1 vol.% H_2, 0.5 vol.% Ne, and the balance He was fed at a rate of 1000 $cm^3 \cdot min^{-1}$ to the catalyst (0.3 g) at 20°C.

The catalytic properties of the samples were examined in an automated installation with a flow reactor using mass-spectrometric analysis of the gas mixture. A catalyst sample with a particle size of 0.25–0.5 mm was mounted in a stainless steel reactor. The catalysts were tested in the oxidation of CO using two variants:

a) under isothermal conditions at 20°C, the reaction mixture containing 100 ppm CO, 1.0 vol.% O_2, 0.5 vol.% Ne, and the balance helium was fed at a rate of 200 $cm^3 \cdot min^{-1}$ to the initial catalyst of volume 0.6 cm^3 cooled to 20°C;

b) under isothermal conditions at 20°C, the reaction mixture containing 100 ppm CO, 1.0 vol.% O_2, 0.5 vol.% Ne, 2.3 vol.% H_2O (which corresponded to the saturated vapor pressure at 20°C), and the balance helium the was fed at a rate of 200 $cm^3 \cdot min^{-1}$ to the initial catalyst of volume 0.6 cm^3 cooled to 20°C.

During the reaction, the concentrations of CO, O_2, CO_2 and H_2O were monitored. The concentrations were measured at a frequency of 0.34 Hz. CO conversion was calculated by the formula $x = (C_{CO}^{inlet} - C_{CO}^{outlet}) / C_{CO}^{inlet}$, where x is the CO conversion, and C_{CO}^{inlet} and C_{CO}^{outlet} are the inlet and outlet concentrations of CO, respectively.

Results

Characterization of the supports and catalysts

The main characteristics of the ferric oxide and hydroxide that were used as a support for the synthesis of Pd-containing catalysts are listed in Table 1.

Table 1. XRD and BET data and Pd loading for of catalysts

Sample	Characteristics of supports				Pd, wt%
	XRD		S_{BET}, $m^2 g^{-1}$	V_{pore}, $cm^3 g^{-1}$	
	Phases	D, nm			
1% Pd(*T*)/Fe_2O_3	α-Fe_2O_3: *a* = 0.5031 nm *c* = 1.374 nm	3.5	50	0.53	1.04
1% Pd(*D*)/Fe_2O_3					1.00
1%Pd(*DF*)/Fe_2O_3					1.00
0.5%Pd(*DF*)/Fe_2O_3					0.51
0.25%Pd(*DF*)/Fe_2O_3					0.25
0.1%Pd(*DF*)/Fe_2O_3					0.10
1%Pd(*DF*)/FeOOH	FeOOH	-	320	0.70	1.01
0.5%Pd(*DF*)/FeOOH					0.50

According to X-ray diffraction analysis, the ferric oxide was α-Fe_2O_3 with lattice parameters a = 0.5031 nm and c = 1.374 nm, and a crystallite size D of 3.5 nm. The specific surface area (S_{BET}) of α-Fe_2O_3 was equal to 50 $m^2 \cdot g^{-1}$, and the pore volume was 0.53 $cm^3 \cdot g^{-1}$. The ferric hydroxide was characterized by S_{BET} equal to 320 $m^2 \cdot g^{-1}$ and a pore volume of 0.70 $cm^3 \cdot g^{-1}$. Therewith, palladium phases in these samples was not detected by XRD; hence, the supported palladium is in a highly dispersed state. At the same time, according to the chemical analysis, the palladium content in the samples varied in the range of 0.1 ÷ 1.0 wt%, which agrees with the specified palladium loading.

Investigation of the catalytic activity in CO oxidation

Fig. 1 demonstrates the dependences of CO conversion vs. time for the catalysts synthesized with ferric oxide and differing in both the conditions of the support treatment and palladium content. The 1%Pd(T)/$Fe_2O_3$was highly active in CO oxidation at room temperature (Fig 1a): initial CO conversion is ~98% in the absence of water vapour in the reaction mixture and ~65% in its presence, and decreases with time in both cases. The obtained results agree with the literature data [16] on the high activity of palladium catalysts supported on ferric oxide in CO oxidation in a "dry" reaction mixture. However, the activity of the 1%Pd(T)/Fe_2O_3 catalyst is much lower in a "wet" mixture and decreases with increasing duration of the experiment.

The 1%Pd(D)/Fe_2O_3 catalyst showed a low activity in CO oxidation (Fig 1b), whereas the 1%Pd(DF)/Fe_2O_3 catalyst demonstrated a high activity. It can be seen (Fig 1c) that in the absence of water in the reaction mixture this catalyst ensured CO conversion at a level of ~95% for 0.5 h, while in the presence of water the CO conversion was ~98% for more than 0.5 h.

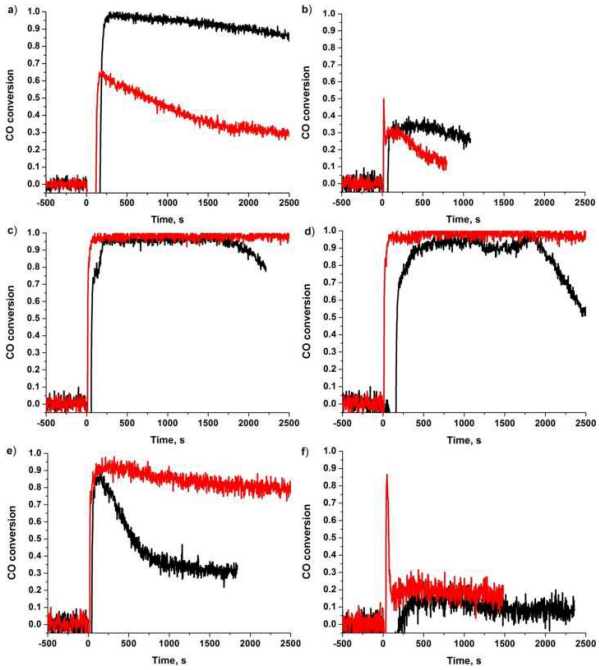

Fig. 1.CO conversion vs. time at 20°C in dry (black curve) and wet (red curve) conditions obtained for 1%Pd(T)/Fe_2O_3 (a), 1%Pd(D)/Fe_2O_3 (b), 1%Pd(DF)/Fe_2O_3 (c), 0.5%Pd(DF)/Fe_2O_3 (d), 0.25%Pd(DF)/Fe_2O_3 (e) and 0.1%Pd(DF)/Fe_2O_3 (f) catalysts.

Moreover, the catalyst synthesized by this method with 0.5 wt% palladium content was also active (Fig 1d): in the presence of water vapor, CO conversion was similar to that observed for the 1%Pd(DF)/Fe_2O_3 catalyst; in the absence of water vapor, CO conversion remained at a level of 93% for

0.3 h and then the catalyst was deactivated. In this case deactivation was faster as compared to the 1%Pd(DF)/Fe_2O_3 catalyst: during the same time (~0.6 h), CO conversion decreased to 78 and 66% for the 1%Pd(DF)/Fe_2O_3 and 0.5%Pd(DF)/Fe_2O_3 catalysts, respectively. A further decrease in palladium content to 0.25 wt.% resulted in a decrease in catalytic activity (Fig. 1e). In the presence of water vapor, CO conversion stabilized near 77%; in the absence of water vapor in the reaction mixture, CO conversion was close to 30%. The 0.1%Pd(DF)/Fe_2O_3 catalyst was found to be inactive (Fig. 1 f). Thus, Pd(DF)/Fe_2O_3 catalysts synthesized by impregnation of the DMF-modified support with a palladium nitrate solution and subsequent treatment with a sodium formate solution and containing (0.5 ÷ 1.0) wt.% Pd are highly active in oxidizing CO at room temperature and ambient humidity.

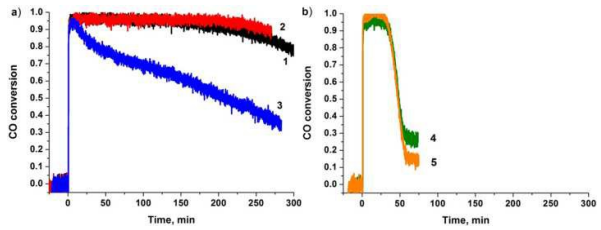

Fig. 2. CO conversion vs. time at 20°C in wet conditions obtained for: a) 1%Pd(DF)/Fe_2O_3 (1), 0.5%Pd(DF)/Fe_2O_3 (2) and 0.25%Pd(DF)/Fe_2O_3 (3); b) 1%Pd(DF)/FeOOH (4) and 0.5%Pd(DF)/FeOOH (5) catalysts.

Note that testing of the catalysts considered above was relatively short-term (0.4 ÷ 0.8 h). So, the most active catalysts were additionally tested for a longer time. It can be seen (Fig. 2a, curve 1) that the 1%Pd(DF)/Fe_2O_3 catalyst ensured a CO conversion of 95%, which was retained for 2.5 h and decreases to 78% in the next 2.5 h. The 0.5%Pd(DF)/Fe_2O_3 catalyst demonstrated the same stability (Fig. 2a, curve 2). The 0.25%Pd(DF)/Fe_2O_3 catalyst was found to be less stable (Fig. 2a, curve 3): the initial CO conversion of 95% decreased linearly and became equal to 35% in 4.5 h.

Replacement of the ferric oxide by ferric hydroxide did not decrease the activity of the Pd(DF)/FeOOH catalyst containing 1.0 or 0.5 wt.% Pd (Fig. 2 b): in the presence of water vapor, CO conversion reached ~95 ÷ 100%. However, these catalysts were less stable: the high CO conversion was retained only for 0.5 h, which was followed by rapid deactivation, and in the next 0.5 h the conversion decreased to 15 ÷ 27% and remained at this level.

Thus, the study demonstrated a relatively high stability of the 1%Pd(DF)/Fe_2O_3 catalyst, which exceeded that of 1%Pd(DF)/FeOOH. Note that decreasing the palladium content to 0.5 wt.% exerted no effect on the stability of the Pd(DF)/Fe_2O_3catalyst.

Taking into account that a decrease in the space velocity makes it possible to increase the detected values of CO conversion [17,18], the 0.5%Pd(DF)/Fe_2O_3 catalyst was tested for oxidation of CO at room temperature and ambient humidity at two space velocities.

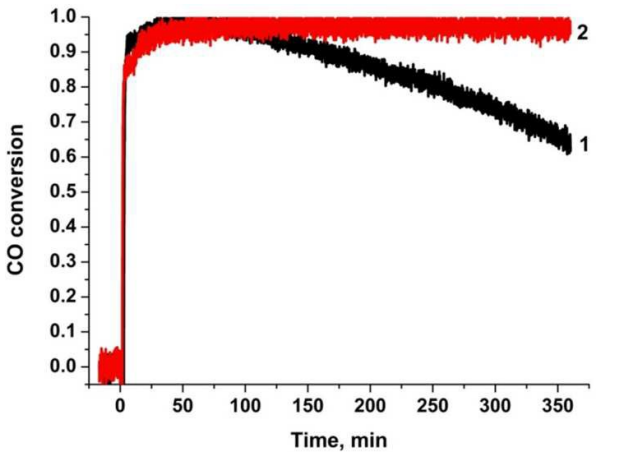

Fig. 3. CO conversion vs. time at 20°C in wet conditions obtained for 0.5%Pd(DF)/Fe_2O_3 catalysts at 20000 h^{-1} (1) and 10000 h^{-1} (2) space velocities.

One can see (Fig. 3) that a two-fold decrease in the space velocity increased the CO conversion value and the catalyst stability: in the initial period CO conversion was 95%, then increased to 100% for 1 h, and remained constant to the end of the experiment (for the next 5 h). Thus, in the presence of the 0.5%Pd(DF)/Fe_2O_3 catalyst the efficiency of CO removal increased with decreasing space velocity of the reaction mixture from 20000 to 10000 h^{-1}.

To elucidate the reasons for the observed differences in activity and stability of the synthesized catalysts, they were studied with the use of H_2-TPR, HRTEM and XPS methods.

Reduction of the catalysts by hydrogen

Fig. 4 shows the time dependence of hydrogen consumption at 20°C on the catalysts. It can be seen that the 1%Pd(D)/Fe_2O_3 catalyst virtually does not consume hydrogen, whereas 1%Pd(DF)/Fe_2O_3 and 1%Pd(DF)/FeOOH, on the contrary, consume it. For the 1%Pd(DF)/Fe_2O_3 catalyst the H_2/Pd ratio is 0.9, while for 1%Pd(DF)/FeOOH it is equal to 25.3. As the theoretical value of H_2/PdO is 1; the obtained value of this ratio may indicate that, along with reduction of a portion of the PdO_x, the reduction of Fe^{3+} to Fe^{2+}occurs in the support, which may be catalyzed by the supported palladium.

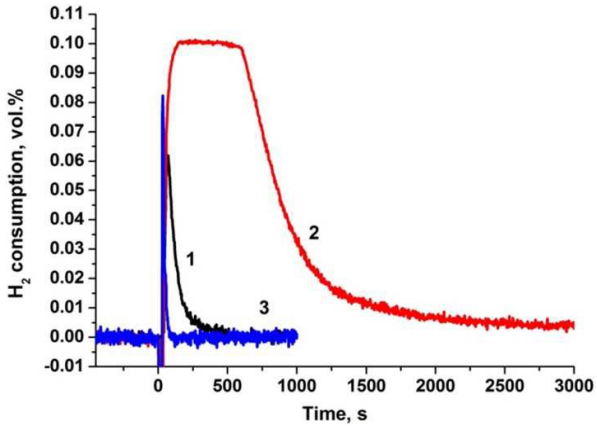

Fig. 4. H_2 consumption vs. time at ambient temperature for 1%Pd(DF)/Fe_2O_3 (1), 1%Pd(DF)/FeOOH (2), 1%Pd(D)/Fe_2O_3 (3) catalysts.

Note that the authors of [16,19] revealed that it is exactly the presence of a noble metal (Pt, Pd, Au) that facilitated the reduction of a support (Fe_2O_3, FeOOH). In particular, H_2 uptake over 1.9% Pd/FeO_x was 1.0 mmol/g, which is 3.7-fold greater than the theoretical amount (0.27 mmol/g). A similar situation was also observed for Au/ferrihydrite [20]. Hence, the reduction process includes not only the palladium oxide states but also the ferric oxide/hydroxide support.

HRTEM study of the catalysts

A TEM study was carried out with the Pd/Fe_2O_3(FeOOH) samples containing 1 wt.% Pd. According to TEM, the Fe_2O_3 support consisted of aggregates ~1 μm in size formed by elongated ~20×50 nm Fe_2O_3 nanoparticles (Fig. 5a). The interplanar spacings measured using Selected Area Electron Diffraction (SAED) obtained from an agglomerate of the Fe_2O_3 particles (Fig. 5 b), correspond to the hematite phase (dn: 0.37, 0.27, 0.25, 0.23 nm, etc., PDF-2, No. 33-0664). The Fe_2O_3 crystals contain defects in the crystal lattice represented by interdomain boundaries; Fig. 5 c displays the HRTEM image for an Fe_2O_3particle containing a defect of this type.

The morphology of the FeOOH support is shown in Fig. 5 d: it is represented by 0.1 ÷ 1 μm aggregates of isometric particles with a size of 5 ÷ 7 nm; the orientation of crystallites in the aggregates is random, which is reflected in the circular SAED pattern (Fig. 5 e). The measured interplanar spacings (dn: 0.47, 0.31, 0.25, 0.22 nm, etc.) correspond to ferrihydrite (PDF-2, No. 29-0712). Fig. 5 f displays an HRTEM image of the FeOOH crystallite lattice with an indication of the interplanar spacings.

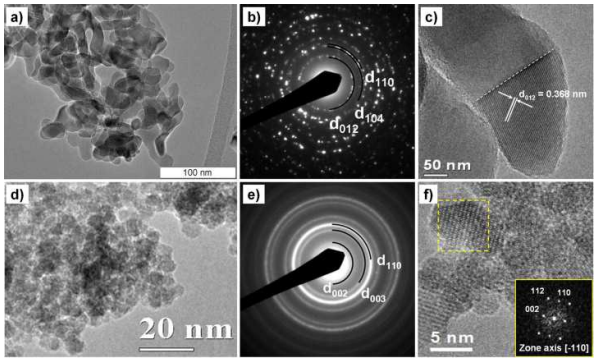

Fig. 5. Fe_2O_3 (a, b, c) and FeOOH (d, e, f) supports: TEM-image of Fe_2O_3 particles (a); SAED pattern obtained from Fe_2O_3 particles agglomerate with reflections corresponding to 0.35 nm [012], 0.25 nm [104], and 0.25 nm [110] distances (b); HRTEM-image of Fe_2O_3 particles with grain boundaries defect marked by dashed line (c); TEM-image of FeOOH particles (d); A SAED pattern obtained from FeOOH particles agglomerate with rings corresponding to 0.47 nm [002], 0.31 nm [003], and 0.25 nm [110] distances (e); HRTEM-image of FeOOH particles with FFT pattern obtained from the area marked by square (f).

The deposition of palladium by the traditional impregnation method leads to the formation of many palladium nanoparticles on the support surface, which are clearly observed in TEM images of the 1%Pd(T)/Fe_2O_3 catalyst (Fig. 6 a). The size distribution of palladium particles is shown in Fig. 6 b; the calculated average size of the palladium nanoparticles is 1.5 nm. Analysis of HRTEM images demonstrates (Fig. 6 c) that the obtained nanoparticles correspond to metallic palladium. Taking into account that the 1%Pd(T)/Fe_2O_3 samples under consideration were not subjected to thermal treatment, it can be supposed that reduction of the ~ 1.5 nm palladium nanoparticles occurs under the action of the electron beam, but the initial state of palladium is the oxidized one.

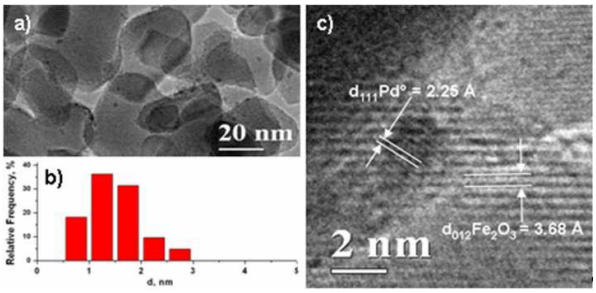

Fig. 6. 1%Pd(T)/Fe_2O_3 catalyst: a) TEM-image; b) histogram of Pd° particles size distruibution; c) HRTEM-image of Pd° nanoparticle supported on Fe_2O_3 particle with corresponding interplanar distances indication.

Pretreatment of the support with a DMF solution strongly affects the dispersity of the supported palladium. Individual palladium nanoparticles with the size of ca. 5 nm can rarely be detected on the support surface in the 1%Pd(D)/Fe_2O_3 sample. The HRTEM image of such a particle is displayed in Fig. 7 a. Interplanar spacings measured on the HRTEM image of this particle correspond to metallic palladium (Fig. 7 b); the presence of palladium was verified by local EDX analysis (Fig. 7 c). We suppose that a main portion of the palladium in this sample is in a highly dispersed state and could not be detected by TEM.

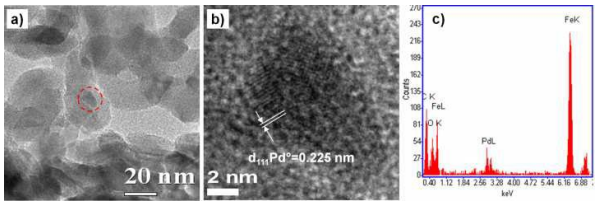

Fig. 7. 1%Pd(D)/Fe_2O_3 catalyst: a) TEM-image; b) HRTEM-image of area marked by circle on fig.(a) with Pd° particle, $d_{111}Pd°$ = 0.225 nm distance marked by arrows; c) EDX spectrum obtained from area marked by circle on fig.(a).

In the 1%Pd(DF)/Fe_2O_3 catalyst, only a small number of palladium nanoparticles was detected in the form of agglomerates (Fig. 8 a). The presence of palladium in agglomerates was confirmed by local EDX analysis (Fig. 8 a, the inset). Analysis of the HRTEM image of the palladium particle revealed that palladium on the particle surface is mostly in a reduced state represented by Pd° (Fig. 8 b, c). In some regions of the image, spacings close to 0.26 ÷ 0.27 nm were detected, which may be related to the presence of a small portion of oxidized PdO crystallites (d_{101}PdO = 0.264 nm). It should be

noted that the size of such aggregate is 30 ÷ 50 nm, while the size of individual Pd° nanodomains is only ~5 nm (Fig. 8 c).

In the 1%Pd(DF)/FeOOH catalyst, agglomerated palladium particles with a similar structure (Fig. 8 d) were found; their size was 20 ÷ 40 nm and the size of individual domains was also equal to ca. 5 nm (Fig. 8 e). The presence of palladium in such agglomerates was verified by EDX analysis (Fig. 8 f). However, the identification of palladium particles from interplanar spacings is complicated because the lattice image overlaps with those of dispersed particles of the FeOOH support.

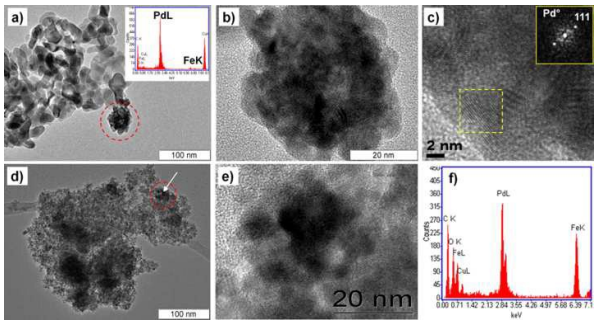

Fig. 8. 1%Pd(DF)/Fe_2O_3 (a, b, c) and 1%Pd(DF)/FeOOH (d, e, f) catalysts: a) TEM-image of 1%Pd(DF)/Fe_2O_3 catalyst with EDX spectrum (inset) obtained from area marked by circle; b, c) HRTEM-images of palladium particle with nanodomain structure marked by circle on fig.(a) and corresponding FFT pattern obtained from area marked by square; d) TEM-image of aggregate from FeOOH particles with supported palladium particles; e) HRTEM-image (e) and corresponding EDX spectrum (f) obtained from area marked by circle on fig.(d).

Note that, although the palladium content in the Pd(DF)/Fe_2O_3 and Pd(DF)/FeOOH samples was 1 wt.%, only minor amounts of such nanodomain palladium aggregates were detected by TEM. This suggests that a portion of the palladium in these catalysts is either in the ionic state or is represented by highly dispersed particles that are undetectable by TEM. Thus,FT-IRand XPS was used to identify the surface states of palladium in the catalysts under consideration.

FT-IR study of the catalysts

Fig. 9A shows the IR spectra of 1%Pd(DF)/Fe_2O_3 sample before and after CO adsorption. Similar IR spectra were observed for 1%Pd(D)/Fe2O3. It can be seen that the spectra contain the absorption bands in the region of1000-1700cm^{-1}characterizing the stretching vibrations in the carbonate and carboxylate structures. The absorption bands at 1330, 1380, and 1460 cm^{-1} can be attributed to the vibrations in the structure of monodentate carbonate. The bands at 1280 and 1530cm^{-1}refer to the asymmetric COO-vibrations of bidentate carbonate [21]. No significant changes in the intensities of the carbonate related bands were observed after the absorption of CO.

Adsorption of CO on 1%Pd(D)/Fe_2O_3 sample resulted in appearance of absorption bands at 1930, 1970, 2095, and 2155 cm^{-1} (Fig. 9B). The band at 1930 cm^{-1} is attributed to bridged-bonded CO on metallic palladium (Pd^0–CO–Pd^0) while the band at 2095 cm^{-1} refers to linearly adsorbed CO on metallic palladium (Pd^0–CO) [22].The band at 1970 cm^{-1} can be ascribed to Pd^+–CO–Pd^+ bridging carbonyls [23]. The low intensity band at 2155 cm^{-1} can be attributed to the adsorption of CO on Pd^{2+} or to physisorbed CO [24]. At low CO exposure, the intensity of the linear adsorption band (2095 cm^{-1}) is higher than that of the bridged one (1930 cm^{-1}), indicating that linear form of CO adsorption is preferential for this sample. This is in consistent with the data published by Qiao et al. [25].

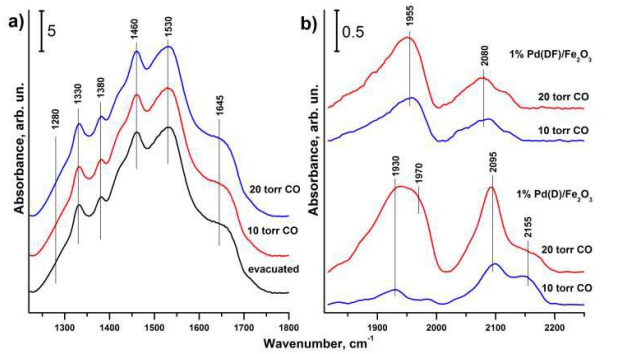

Fig. 9.a) FTIR spectra of 1%Pd(DF)/Fe_2O_3obtained after air evacuation and after CO adsorption at 10 and 20 torr. b) Difference spectra obtained for 1%Pd(DF)/Fe_2O_3 and 1%Pd(D)/Fe_2O_3samples after CO adsorption at 10 and 20 torr.

The intensity of the bands at 1930, 1970, and 2095 cm^{-1} increases with the increase in CO pressure, while the 2155 cm^{-1} band intensity decreases strongly indicating virtually complete reduction of Pd^+. CO adsorption on 1%Pd(DF)/Fe_2O_3 sample leads to appearance of bands at 1955 and 2080 cm^{-1} related to bridged-bonded and linearly-bonded CO on metallic palladium, respectively (Fig. 9B). A small shoulder at 2118 cm^{-1} can be attributed to Pd^+–CO linear complexes. The intensity ratio of bridged/linear CO adsorption corresponds to CO adsorption on small Pd clusters in accordance with [26]. Increase of CO pressure does not affect on the shape of IR spectrum for 1%Pd(DF)/Fe_2O_3 sample, i.e, intensity ratio of brigded/linear CO adsorption does not change. These observations allow us to conclude that oxidized Pd-species initially present in 1%Pd(D)/Fe2O3 catalysts and these species reduces to metallic Pd-clusters under CO action. On the contrary, reduced metallic Pd clusters present initially in the 1%Pd(DF)/Fe_2O_3 sample.

XPS study of the catalysts

Table 2 lists the surface compositions of the 1%Pd(T)/Fe_2O_3, 1%Pd(D)/Fe_2O_3, 1%Pd(DF)/Fe_2O_3 and 1%Pd(DF)/FeOOH catalysts determined by XPS. In addition to the main elements, nitrogen is also present on the surface. The O/Fe ratio on the surface of 1%Pd(D)/Fe_2O_3, 1%Pd(DF)/Fe_2O_3 samples corresponds to the calculated value (Table 1), while in the 1%Pd(T)/Fe_2O_3 and 1%Pd(DF)/FeOOH samples this ratio is much higher, probably due to a substantial contribution of oxygen from surface nitrate and hydroxide groups, which is confirmed by the high N/Fe ratio in these samples. The palladium content with respect to iron on the catalyst surface is also different: for the 1%Pd(T)/Fe_2O_3 catalyst it is 3%. Higher Pd concentration compared with it expected value (0.8% atomic) observed for this catalyst is due to its surface localization. Pd concentration observed for the other catalysts is an order of magnitude lower (Table 2), which could be

explained by morphological effects. Pd-species could be presumably distributed within the interdomain boundaries of the support. The main state of iron on the surface of the samples (Fig. 10) is characterized by $E_b(Fe2p_{3/2})$ = 710.6 eV, which corresponds to Fe^{3+} [27].

Table 2. Surface composition of the catalyst obtained by XPS

Sample	Atomic concentration of elements on surface determined by XPS, at.%								
	Fe	O	Pd	C	N	O/Fe	Pd/Fe	N/Pd	N/Fe
1%Pd(*T*)/Fe_2O_3	26	52	0.84	19	1.8	200	3	220	7
1%Pd(*D*)/Fe_2O_3	33	50	0.15	16	0.5	150	0.5	330	1.5
1%Pd(*DF*)/Fe_2O_3	30	48	0.08	21	0.5	160	0.27	650	1.7
1%Pd(*DF*)/FeOOH	21	43	0.045	35	0.8	200	0.21	1750	3.7

The samples containing Fe_2O_3 are characterized by the presence of satellites with a binding energy close to 720 eV, while in the Fe2p spectrum of 1%Pd(DF)/FeOOH such satellites are absent. This indicates that, along with Fe^{3+}, Fe^{2+} is also present on the surface of the 1%Pd(DF)/FeOOH catalyst [27]. Hence, the surface of the 1%Pd(DF)/FeOOH catalyst is substantially reduced. This result agrees well with the H_2-reduction data (Fig. 4) indicating that deep reduction of the support was possible only with this catalyst. In the 1%Pd(T)/Fe_2O_3 sample, nitrogen is in two states with E_b(N1s) = 406.4 and 403.8 eV (Fig. 9), corresponding to nitrates and nitrites, respectively [14]. Since a high concentration of NO^{3-} groups is observed on the catalyst surface, and taking into account the ratio N/Pd = 2.2, it can be supposed that the palladium on the support surface is present mostly as a nitrate, which corresponds to the synthesis procedure. In the other samples, nitrogen was detected in much smaller amounts and in a state with E_b(N1s) = 398.5 ÷ 400.5 eV, which is typical for nitrogen in organic nitrogen-containing compounds, e.g. in DMF [14]. Fig. 11 shows the Pd3d lines characterizing the state of palladium in the catalysts under consideration.

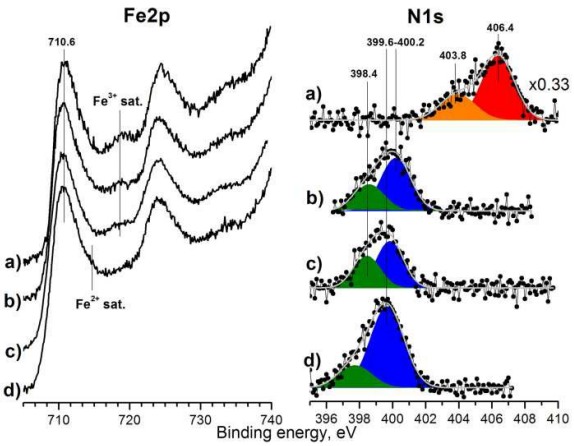

Fig. 10. Fe2p XP-spectra and N1s XP-spectra with subtracted Shirley background and curve-fitting by individual pseudo-Voigt components for 1%Pd(T)/Fe_2O_3 (a), 1%Pd(D)/Fe_2O_3 (b), 1%Pd(DF)/Fe_2O_3 (c) and 1%Pd(DF)/FeOOH (d). (N1s spectrum for 1%Pd(T)/Fe_2O_3 catalyst was 3-fold decreased for clarity).

In the 1%Pd(T)/Fe_2O_3 sample, the palladium is oxidized (Fig. 11 a) and represented by two states: a component with $E_b(Pd3d_{5/2})$ = 338.0 eV corresponds to Pd^{2+} in nitrate palladium complexes [28], while an additional state with $E_b(Pd3d_{5/2})$ = 337.0 eV corresponds to PdO [29,30].

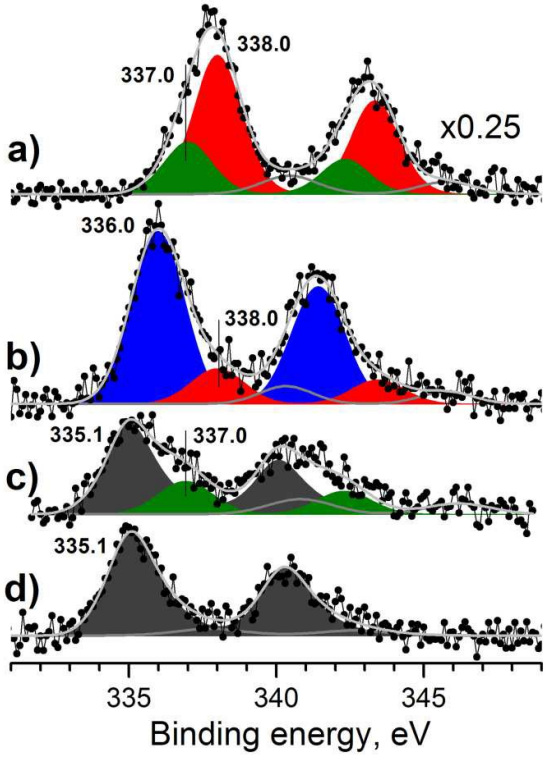

Fig. 11. Pd3d XP-spectra with subtracted Shirley background and curve-fitting by individual pseudo-Voigt doublet components for 1%Pd(T)/Fe_2O_3 (a), 1%Pd(D)/Fe_2O_3 (b), 1%Pd(DF)/Fe_2O_3 (c) and 1%Pd(DF)/FeOOH (d). (Pd3d spectrum for 1%Pd(T)/Fe_2O_3 catalyst was 4-fold decreased for clarity).

The binding energy of the main state of palladium in 1%Pd(D)/Fe_2O_3 is 336.0 eV (Fig. 11 b) and lies between two values: the first one is typical of PdO, $E_b(Pd3d_{5/2})$ = 336.7 ÷ 337.0 eV [29,30], and the second one characterizes metallic palladium, $E_b(Pd3d_{5/2})$ = 335.1 ÷ 335.4 eV [29,31]. This state of palladium

can be attributed to small palladium clusters deposited on various supports [32,33]. In this case, the shift in the Pd3d level toward high binding energies is caused by changes in physical relaxation processes during photoionization due to changes in the electronic structure of metal clusters in comparison with the bulk metal. These clusters, probably, were formed from initial Pd^{2+}-DMF complexes, which were unstable under X-ray exposure in UHV conditions. The relatively low intensity of the palladium state with $E_b(Pd3d_{5/2})$ = 336.0 eV can be explained by intercalation of these clusters under the DMF layer and their interaction with the Fe_2O_3 support; thus, the photoelectrons emitted from these clusters are attenuated by the topmost DMF layer. An additional low intensity state with $E_b(Pd3d_{5/2})$ = 338.0 eV originated from residual Pd^{2+}-DMF complexes not decomposed during XPS measurement. According to the XPS data reported in [34], fine palladium nanoparticles covered by an organic polymer matrix are characterized by $E_b(Pd3d_{5/2})$ = 335.8 eV, which is very close to the binding energy obtained in this work.
In the 1%Pd(DF)/Fe_2O_3 (Fig. 11 c) and 1%Pd(DF)/FeOOH samples (Fig. 11 d), the main state of palladium with $E_b(Pd3d_{5/2})$ = 335.1 eV corresponds to metallic palladium. The 1%Pd(DF)/Fe_2O_3 sample (Fig. 11 c) has an additional state with $E_b(Pd3d_{5/2})$ = 337.0 eV corresponding to PdO.
Thus, the XPS data allows us to conclude that the state of palladium on the surface of the Pd/Fe_2O_3 catalysts is determined mainly by the conditions of the support treatment with organic compounds.

Discussion

It is known [20,35] that FeO_x is able to adsorb and activate oxygen on its surface, and this property is strongly enhanced by the synergetic effect caused by the presence of a noble metal. As shown in [20], surface redox of the FeO_x support takes place easily at room temperature with the assistance of Pd, so Pd/FeO_x catalysts can convert CO to CO_2 completely at room temperature.
Indeed, the Pd/Fe_2O_3catalysts synthesized in this work are also active in CO oxidation at room temperature. However, their activity was found to depend on the preparation procedure employed for deposition of the active component and on its content. Thus, the 1%Pd(*T*)/Fe_2O_3 catalyst synthesized by the traditional method is highly active in the oxidation of CO at room temperature in a "dry" reaction mixture: in the first minutes, CO conversion reaches ~98% and then gradually decreases (Fig.1a). However, this catalyst proved to have low efficiency in the presence of water vapor, which may be related either to the condensation of water in mesopores of the hydrophilic support at room temperature or to the formation of carbonates that block the active surface sites.
To increase the hydrophobicity of the support, a carbon-containing component represented by DMF – $HCON(CH_3)_2$ with two hydrophobic groups was deposited on the support surface. However, the 1%Pd(*D*)/Fe_2O_3 catalyst synthesized by palladium deposition on this modified support was inactive in CO oxidation at room temperature (Fig. 1b). Only the introduction of the reduction step in which the catalyst was treated by a sodium formate solution with subsequent removal of sodium admixtures by washing resulted in the formation of active catalysts (Fig. 1c). Thus, the (0.5-1.0)%Pd(*DF*)/Fe_2O_3(FeOOH) catalysts ensure virtually 100% conversion of 100 ppm CO at room temperature, both in the presence and absence of water vapor. Reaction rates and TOF values were calculated at conversion lower 20%(Fig. S1). At this case reagents concentration along the catalyst bed could be considered to be near constant and the plug flow reactor could be considered as a continuous stirred tank reactor (CSTR) [1-4], which allows us to use the equations of reaction rates. Calculation of TOF using FTIR spectroscopy considering all bridged and linear adsorbed species gives value (0.050±0.015 s^{-1}) which is close to values obtained using XPS (0.035 s^{-1}). Detailed description of TOF estimation procedures presented in Supplementary Information.

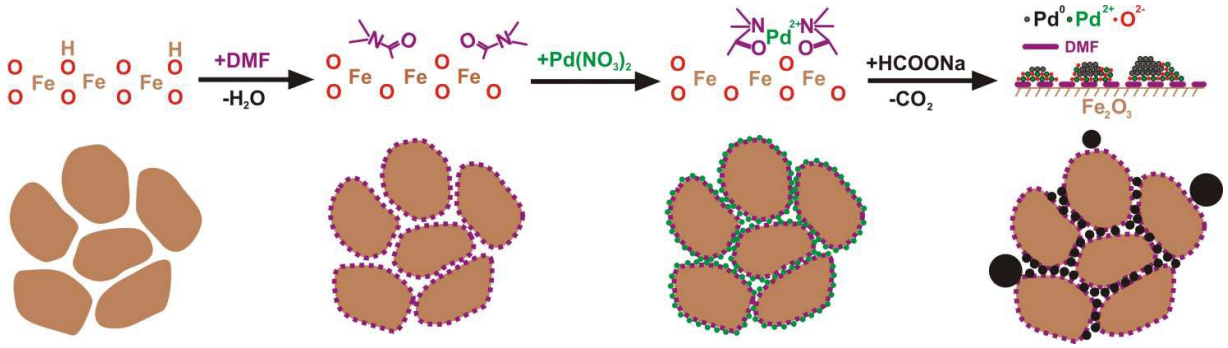

Fig. 12. Proposed scheme of formation Pd(DF)/Fe_2O_3, and Pd(DF)/FeOOH catalyst microstructure during preparation.

Decreasing the palladium content to 0.25–0.1 wt.% decreased the activity, probably due to the low surface concentration of palladium. The observed differences in the activity of Pd(*T*)/Fe_2O_3, Pd(*D*)/Fe_2O_3, Pd(*DF*)/Fe_2O_3 and Pd(*DF*)/FeOOH catalysts containing 1 wt.% Pd in CO oxidation at room temperature are caused by different states and dispersions of palladium.

According to the TEM data, the particles of supported palladium in the 1%Pd(*T*)/Fe_2O_3 catalyst are represented by metal nanoparticles with an average size of ~ 1.5 nm. As was demonstrated [28], such highly dispersed palladium nanoparticles are quite active in low-temperature oxidation of CO.

Accoding to the XPS data, the palladium in this catalyst is represented by two states: the main state with $E_b(Pd3d_{5/2})$ = 338.0 eV corresponding to nitrates, and an additional state PdO with $E_b(Pd3d_{5/2})$ = 337.0 eV. The disagreement between the TEM and XPS results can be explained bythe reduction of palladium nitrates under the action of the electron beam, leading to the formation of highly dispersed metal nanoparticles. In turn, this indicates an easy reduction of the highly dispersed ionic state of palladium in this catalyst, which is likely to occur under the conditions of CO oxidation, thus conferring the high activity of the catalyst when the reaction is carried out in a "dry" reaction mixture.

In the 1%Pd(*D*)/Fe_2O_3 catalyst, palladium is also present in the highly dispersed state; only individual palladium nanoparticles ~ 5 nm in size can rarely be detected by TEM on the support surface. The small number of detectable palladium nanoparticles (*at the identical palladium content*) may indicate the existence of highly dispersed palladium species that are hard to detect by this method. Most probably, the DMF layer interacts strongly with palladium and hinders the formation of metallic Pd nanoparticles detectable by TEM in this case, so only minor Pd-clusters could form during reduction by the e-beam. Such strong interaction leads to the formation of DMF-Pd complexes, which are proposed to be inactive in the CO oxidation reaction. This assumption is confirmed by the next facts: this catalyst is irreducible in the mixture of 0.1% hydrogen in He at 20°C (fig.4). According to FTIRS CO is adsorbed only on oxidized Pd-species observed initially in this catalyst at 10 torr CO pressure. Only increase in CO pressure up to 20 torr leads to formation of reduced Pd-clusters (fig.9.b). Thus, the palladium state in 1%Pd(*D*)/Fe_2O_3 catalyst under reaction mixture (100 ppm CO, 1.0 vol.% O_2 in He) is most probably remains oxidized.Having the main portion of its oxidized palladium bound up with the DMF layer, the 1%Pd(*D*)/Fe_2O_3 catalyst possesses very low catalytic activity in CO oxidation(fig.1.b).

TPR-H_2 experiment was carried out using 1%Pd(*D*)/Fe_2O_3 catalyst in order to reduce Pd^{2+}-DMF complexes by other way. After the reduction with H_2 the 1%Pd(D)/Fe_2O_3catalyst was cooled in helium. The obtained catalyst was tested in CO oxidation at the same conditions as in experimental part.

The obtained catalyst was characterized by high activity in dry conditions for about 20 minutes, then the conversion was observed to decrease slowly. In wet conditions the catalyst deactivates more rapidly. Thus, reduction with sodium formate allowed us to reduce the Pd^{2+} species without affecting the hydrophobic DMF layer, which leads to active and stable in wet ambient CO oxidation catalysts. The detailed information is presented in Supporting Information.

According to the scheme of catalyst synthesis presented in Fig. 12, introducing the step in which the samples are treated with sodium formate solution as the mild reductant changes the state of the palladium in 1%Pd(*DF*)/Fe_2O_3 and 1%Pd(*DF*)/FeOOH as compared to 1%Pd(*D*)/Fe_2O_3. As a result of such treatment, the main state of palladium becomes reduced. FTIR spectroscopy reveals CO adsorption on the metallic Pd-clusters (fig.9.b) in 1%Pd(*DF*)/Fe_2O_3 catalyst. Palladium state 1%Pd(*DF*)/Fe_2O_3 and 1%Pd(*DF*)/FeOOH catalysts, according to XPS, is the metallic one with $E_b(Pd3d_{5/2})$ = 335.1 eV, and the additional state is PdO. However, the palladium content with respect to iron on the surface of these catalysts is 0.21 ÷ 0.27 at.% (Table 1), which is twice as low as the value for the 1%Pd(*D*)/Fe_2O_3 catalyst before treatment by formate. This can be explained by aggregation of some portion of the palladium during reduction. This is confirmed by the TEM data showing small amounts of palladium aggregates in the 1%Pd(*DF*)/Fe_2O_3 and 1%Pd(*DF*)/FeOOH samples. It should be noted that the state of the nitrogen residing on the surface of the 1%Pd(*DF*)/Fe_2O_3(*FeOOH*) catalysts is the same as on the surface of 1%Pd(*D*)/Fe_2O_3; hence, DMF is retained after the treatment with sodium formate solution.

A set of the indicated data suggests that a great portion of the palladium in these catalysts remains in a highly dispersed state after reduction in the form of small palladium clusters presumably distributed within the interdomain boundaries of the support. In turn, the presence of highly dispersed palladium clusters [28] in combination with PdO_x, which is characterized by an easy $Pd^{2+}\leftrightarrow Pd^{\delta+}$ transition [36,37] confirmed by the reduction of the samples at the room temperature, provides the high activity of the 1%Pd(*DF*)/Fe_2O_3(*FeOOH*) catalysts in CO oxidation at room temperature both in the presence and absence of water vapor. Noteworthy is the fact that the presence of a carbon-containing component confers hydrophobic properties to the surface, thus increasing the catalyst's stability in the presence of water vapor. In addition, the high activity of the Pd(*DF*)/FeOOH catalyst can also be related to the easy $Fe^{3+}\rightarrow Fe^{2+}$ reduction of the support at room temperature; the synergetic effect of the $Pd^{2+}/Pd^{\delta+}$ and Fe^{3+}/Fe^{2+} redox pairs produces an increased mobility of the catalyst oxygen.

According to the data reported in [8], the supports consist of ferric hydroxide and oxide and contain a large number of OH groups, which are important and favorable for CO oxidation. In addition, as regards supported Pd catalysts, Golunski et al. [38] had found that the activity of ferric oxide supported Pd catalysts for CO oxidation could be dramatically enhanced by a short low-temperature exposure to hydrogen without any subsequent thermal treatment, which is mainly related to the large amount of OH derived from the H_2 treatment instead of the reduction of Pd^{2+} ions to metallic Pd. Such an opinion as to the role of hydroxyl groups in the low-temperature oxidation of CO was also proposed in [39]: CO can directly interact with surface hydroxyl groups to form the intermediates: CO_{ad} + $[OH]_s\rightarrow [COOH]_s$; in turn, $[COOH]_s + [O]_s\rightarrow CO_2 + [OH]_s$.

When CO oxidation at room temperature is performed in the presence of water vapor (CO, O_2 and H_2O) on Pd(*DF*)/Fe_2O_3 catalysts, an increase in their activity is observed. This may be

caused by the effect of water on the formation of intermediates; in particular, water can promote the decomposition of intermediates produced by the interaction with CO, thus liberating the active sites. In addition, according to [39], the presence of water in the reaction mixture facilitates the formation of hydroxyl groups according to the reaction $O_2 + H_2O \rightarrow [O]_s + 2OH^-$. According to [40,41], hydroxyl groups are better oxidants as compared to oxygen. And finally, the presence of water leads to the formation of hydroxyl groups on the catalyst surface, which results in a decrease in CO–Pd strength and makes it possible to produce either CO_2 or carbonate species [42].

Conclusions

The state and dispersion of palladium in $Pd/Fe_2O_3(FeOOH)$ catalysts that differ in their preparation procedure, content and properties of the iron-containing support, as well as their relationship with CO oxidation activity at room temperature both in the presence and absence of water vapor in the reaction mixture have been studied.

It was shown that palladium in the 1wt.%$Pd(T)/Fe_2O_3$ catalyst synthesized by traditional impregnation is mostly in the ionic state, which can easily be reduced to form particles ~ 1.5 nm in size. This enables a high activity of the catalyst in CO oxidation at room temperature performed in a "dry" reaction mixture. However, the catalyst has only low activity in the presence of water vapor, either due to its condensation in mesopores of the hydrophilic support at room temperature or due to the formation of carbonates that block the active surface sites.

In the 1wt.%$Pd(D)/Fe_2O_3$ catalyst synthesized using the DMF-modified support, palladium is represented by highly dispersed Pd-DMF complexes that are irreducible by hydrogen at room temperature and inactive in the CO oxidation reaction under the given conditions.

On the surface of $(0.5 \div 1.0)$ wt. %$Pd(DF)/Fe_2O_3(FeOOH)$ catalysts, which were synthesized by impregnation of the DMF-modified support with a palladium nitrate solution and subsequent reduction by sodium formate solution, palladium is represented by highly dispersed metal clusters supposedly distributed within the interdomain boundaries of the support and a small amount of Pd^o and PdO nanoparticles. Such palladium species provide 100% CO conversion at room temperature and ambient humidity for a long time. In addition, the stability of the $(0.5 \div 1.0)$ wt.% $Pd(DF)/Fe_2O_3$ catalysts increased when the space velocity of the reaction mixture was decrease from 20000 to 10000 h^{-1}.

Acknowledgements

The work was supported by the Ministry of Education and Science of the Russian Federation. We are grateful to V.I. Zaikovskii for useful discussion. This work was supported by the Skolkovo Foundation (Grant Agreement for Russian educational organizations no. 3 of December 25.2014).

References

1 O.S.H. Administration, Carbon Monoxide, Exposure Limits, *Occupational Safety & Health Administration U.S. Department of Labor*, https://www.osha.gov/dts/chemicalsampling/data/CH_225600.html.
2 Cosmonaut's habitable environments on board of manned spacecraft. General medicotechnical requirements. Russian Federation Government Standard. 1.07.1996 http://docs.cntd.ru/document/gost-r-50804-95.
3 M. Haruta, N. Yamada, T. Kobayashi, S. Iijima, *Journal of Catalysis,* 1989, **115**, 301-309.
4 M. Khoudiakov, M.C. Gupta, S. Deevi, *Applied Catalysis A: General*, 2005, **291**, 151-161.
5 M. Haruta, *Gold Bull*, 2004, **37**, 27-36.
6 M. Haruta, *CATTECH*, 2002, **6**, 102-115.
7 M.-F. Luo, Z.-Y. Hou, X.-X. Yuan, X.-M. Zheng, *Catalysis Letters*, 1998, **50**, 205-209.
8 B. Qiao, L. Liu, J. Zhang, Y. Deng, *Journal of Catalysis*, 2009, **261**, 241-244.
9 H.H. Kung, M.C. Kung, C.K. Costello, *Journal of Catalysis*2003, **216**, 425-432.
10 W.J. Price, *Analytical Atomic Absorption Spectroscopy, Heyden& Son Ltd.*, London-New York-Rheine, 1972.
11 N.I. Baklanova, A.T. Titov, A.I. Boronin, S.V. Kosheev, *Journal of the European Ceramic Society*, 2006, **26**, 1725-1736.
12 A.S. Ivanova, E.M. Slavinskaya, R.V. Gulyaev, V.I. Zaikovskii, O.A. Stonkus, I.G. Danilova, L.M. Plyasova, I.A. Polukhina, A.I. Boronin, *Applied Catalysis B: Environmental*, 2010, 97, 57-71.
13 R.V. Gulyaev, S.V. Koscheev, S.E. Malykhin, *Journal of Electron Spectroscopy and Related Phenomena*, 2015, **202**, 89-101.
14 J.F. Moulder, W.F. Strickle, P.E. Sobol, K.D. Bomben (Eds.), *Handbook of X-ray Photoelectron Spectroscopy*, Perkin-Elmer Corporation, Physical Electronics Division, Minnesota, 1992.
15 S. Lowell, J.E. Shields, M.A. Thomas, M. Thommes, *Characterization of Porous Solids and Powders: Surface Area, Pore Size and Density*, Springer Netherlands, 2004.
16 L. Liu, F. Zhou, L. Wang, X. Qi, F. Shi, Y. Deng, *Journal of Catalysis*, 2010, **274**, 1-10.
17 S. Li, G. Liu, H. Lian, M. Jia, G. Zhao, D. Jiang, W. Zhang, *Catalysis Communications*, 2008, **9**, 1045-1049.
18 J. Deng, L. Zhang, H. Dai, H. He, C.T. Au, *Applied Catalysis B: Environmental*, 2009, **89**, 87-96.
19 K. Zhao, H. Tang, B. Qiao, L. Li, J. Wang, *ACS Catalysis*, 2015, **5**, 3528-3539.
20 L. Li, A. Wang, B. Qiao, J. Lin, Y. Huang, X. Wang, T. Zhang, *Journal of Catalysis* 2013, **299**, 90-100.
21 A. Davydov, Molecular spectroscopy of oxide catalyst surfaces, Wiley: Chichester, 2003, England.
22 G. Rupprechter, H. Unterhalt, M. Morkel, P. Galletto, L. Hu, H.-J. Freund,*Surface Science 2002,* **502-503,** *109-122.*
23 D. Tessier, A. Rakai, F. Bozon-Verduraz*, J. Chem. Soc. Faraday Trans.* 1992, **88,** 741-749
24 P. Kast, M. Friedrich, D. Teschner, F. Girgsdies, T. Lunkenbein, R. Naumann d'Alnoncourt, M. Behrens, R. Schlögl, *Applied Catalysis A: General*, 2015, **502**, 8-17.
25 B. Qiao, J. Lin, L. Li, A. Wang, J. Liu, T. Zhang, *ChemCatChem.* 2014, **6**, 547-554.
26 J. B. Giorgi, T. Schroeder, M. Baumer, H.-J. Freund, Surface Science, 2002, **498,** L71–L77.
27 D.D. Hawn, B.M. Dekoven, *Surf. Interface Anal.,*1987, 10, 63-74.
28 R.V. Gulyaev, A.I. Stadnichenko, E.M. Slavinskaya, A.S. Ivanova, S.V. Koscheev, A.I. Boronin, *Applied Catalysis A: General*,2012, **439–440**, 41-50.

29 T. Pillo, R. Zimmermann, P. Steiner, S. Hüfner, *Journal of Physics: Condensed Matter*, 1997, **9**, 3987.
30 A.I. Boronin, E.M. Slavinskaya, I.G. Danilova, R.V. Gulyaev, Y.I. Amosov, P.A. Kuznetsov, I.A. Polukhina, S.V. Koscheev, V.I. Zaikovskii, A.S. Noskov, *Catalysis Today*, 2009, **144**, 201-211.
31 G.B. Hoflund, H.A.E. Hagelin, J.F. Weaver, G.N. Salaita, *Applied Surface Science*, 2003, **205**, 102-112.
32 G.K. Wertheim, *Zeitschrift für Physik D Atoms, Moleculesand Clusters*,1989, 12, 319-326.
33 M.G. Mason, *Physical Review B*,1983, **27**, 748-762.
34 J. García-Aguilar, I. Miguel-García, Á. Berenguer-Murcia, D. Cazorla-Amorós, *Carbon*,2014, **66**, 599-611.
35 L. Liu, B. Qiao, Y. He, F. Zhou, B. Yang, Y. Deng, *Journal of Catalysis*, 2012,**294**, 29-36.
36 S.-H. Oh, G.B. Hoflund, *Journal of Catalysis*, 2007, **245**, 35-44.
37 S.F. Parker, *Chemical Communications*,2011, **47**, 1988-1990.
38 S. Golunski, R. Rajaram, N. Hodge, G.J. Hutchings, C.J. Kiely, *Catalysis Today*,2002, **72**, 107-113.
39 S. Zhang, X.-S. Li, B. Chen, X. Zhu, C. Shi, A.-M. Zhu, *ACS Catalysis*,2014, **4**, 3481-3489.
40 A. Manasilp, E. Gulari, *Applied Catalysis B: Environmental*, 2002, **37**, 17-25.
41 A. Parinyaswan, S. Pongstabodee, A. Luengnaruemitchai, *International Journal of Hydrogen Energy*,2006, **31**, 1942-1949.
42 Z.M. El-Bahy, A.I. Hanafy, M.M. Ibrahim, M. Anpo, *Journal of Molecular Catalysis A: Chemical*,2011, **344**, 111-121.

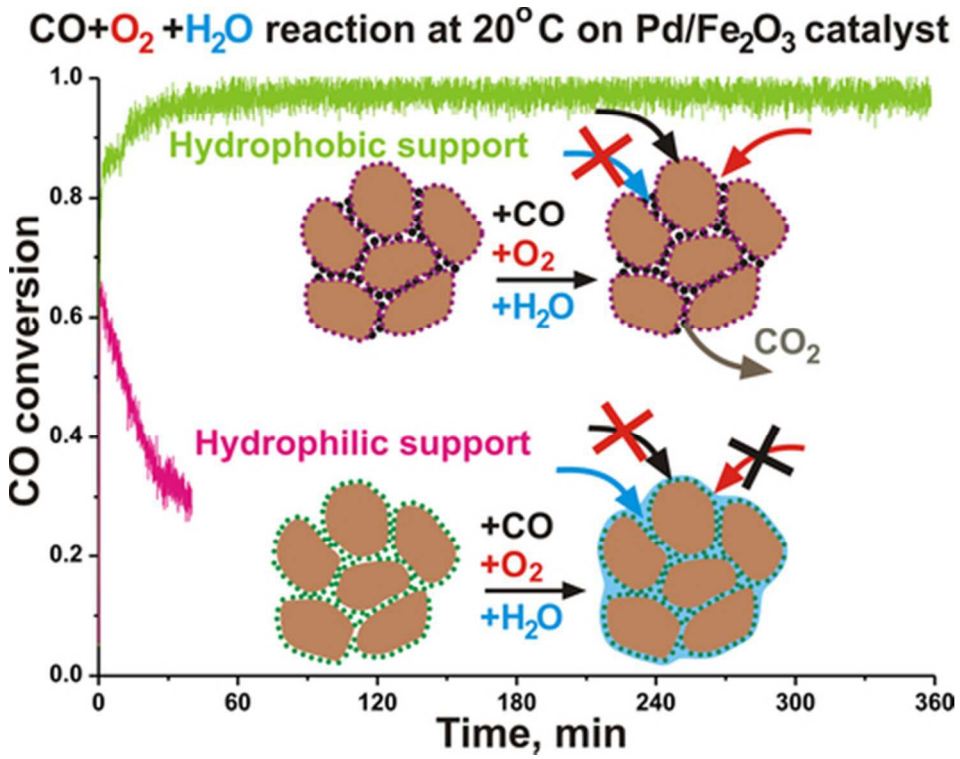

Scheme of the catalysts preparation and its activity in CO oxidation at ambient temperature and humidity
39x31mm (300 x 300 DPI)